ACS APPLIED MATERIALS & INTERFACES

Letter

www.acsami.org

Engineering Controllable Architecture in Matrigel for 3D Cell Alignment

Jae Myung Jang,[†,§] Si-Hoai-Trung Tran,[‡,§] Sang Cheol Na,[‡] and Noo Li Jeon*[,†,‡]

[†]Interdisciplinary Program in Neuroscience and [‡]School of Mechanical and Aerospace Engineering, Seoul National University, Seoul, Republic of Korea

Supporting Information

ABSTRACT: We report a microfluidic approach to impart alignment in ECM components in 3D hydrogels by continuously applying fluid flow across the bulk gel during the gelation process. The microfluidic device where each channel can be independently filled was tilted at 90° to generate continuous flow across the Matrigel as it gelled. The presence of flow helped that more than 70% of ECM components were oriented along the direction of flow, compared with randomly cross-linked Matrigel. Following the oriented ECM components, primary rat cortical neurons and mouse neural stem cells showed oriented outgrowth of neuronal processes within the 3D Matrigel matrix.

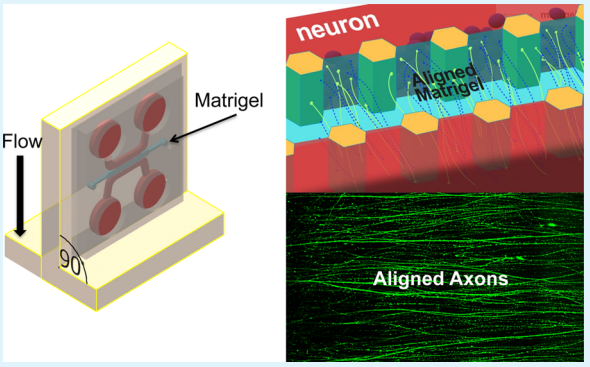

KEYWORDS: *microfluidics, 3D cell culture, aligned hydrogel, shear flow, ECM*

The extracellular matrix (ECM) is a complex environment consisting of proteins, proteoglycans, and other biochemical molecules. The ECM provides structural support for cells,[1] influences cell fate,[2] and regulates cell growth[3] and development.[4] Therefore, the use of reconstituted ECM is a key feature in the realization of in vitro models of normal cell functions. However, native ECM is extremely thin,[5] such that it has been difficult to directly apply in vitro models and to study its composition, structure, and function. Therefore, over the past decade, many studies have shown the possibility of mimicking the native ECM in in vitro cell culture by using a variety of hydrogels,[6−8] taking advantage of their high water content and mechanical properties to replicate those of tissues in vivo.

In this light, engineering ECM with ordered functional structures is an attractive prospect. The formation of patterned hydrogels has been the subject of several investigations. Major efforts have been invested in fabricating three-dimensional scaffolds with the help of heat,[9] light,[10,11] molding,[12] and nanoimprinting,[13] followed by bioprinters.[14] Techniques of building multilayered gel scaffolds, such as layer-by-layer stereolithography,[15] have also been applied toward three-dimensionally patterned hydrogels.[16] Furthermore, two-photon laser scanning photolithography has recently enabled a postgelation process following the initial gelation of a preformed hydrogel only at the focal point.[17] Contrary to these, patterning methods involving self-polymerization, which require physical modification of gel structures during gelation, have been introduced in a wide range of techniques. Such investigations have attempted to reconstitute hydrogel structures using various methods including electro-spinning,[18] exposure to strong magnetic fields[19] or electrical gradients,[20] prompt pressure-driven flow[21,22] or hydrodynamic flow through a microfluidic device,[23] combinations of fluid flow and magnetic fields,[24,25] dip-pen nanolithography,[26] and freezing and thawing.[27] Collagen fibril orientation has recently been applied in the alignment of astrocytes[28] and neurons[29] in three-dimensional (3D) gels with the technique of unidirectional draining during the gelation of collagen solutions. However, despite the development of these techniques, the alignment of ECM components does not only demand complicated steps, but the application of these techniques to Matrigel is also rare while the alignment technique can be applied to various other hydrogels. Moreover, the 3D patterning of hydrogels lacks specific realization, and is still at an initial stage of development.

In this study, we used microfluidic techniques of constraining independent hydrogels and generating continuous flow to test whether fluid flow-induced shear stress mediated 3D Matrigel alignment. Figure 1a shows a photograph of the microfluidic device used in this work. The microfluidic device was fabricated with polydimethylsiloxane using soft lithography. The design contains three separate channels separated by an array of hexagonal pillars as described previously.[30] The main function of the pillars was to allow selective filling of each channel independently by engineering the capillary burst pressure. The main channel in the middle was used in the 3D hydrogel and

Received: November 25, 2014
Accepted: January 14, 2015
Published: January 14, 2015

DOI: 10.1021/am508292t
ACS Appl. Mater. Interfaces 2015, 7, 2183−2188

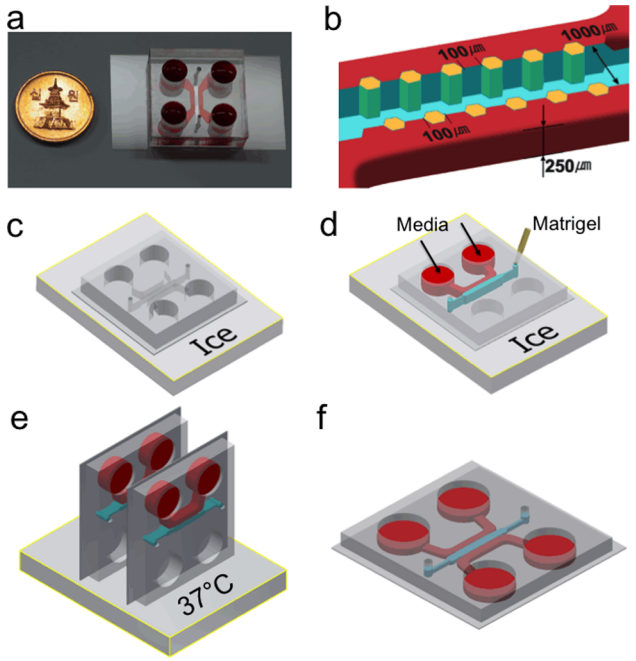

Figure 1. Schematic diagram of the experimental steps for flow-induced hydrogel alignment in a microfluidic device. (a) The entire microfluidic device was about 1″ × 1″ in size. (b) The device contained three separate microchannels (1000 μm wide, 250 μm high) separated by an array of posts that allowed selective filling of each channel with different gels or media. (c) The microfluidic device and hydrogel were placed on ice (T = 4 °C) to maintain the hydrogel at the liquid state. (d) First, the middle channel was loaded with non-cross-linked Matrigel. Before the Matrigel solidified, media was added to the left channel and the entire device was tilted at 90°. (e) The microfluidic device was placed in an incubator (T = 37 °C) for 1 h while the Matrigel solidified. Media continuously percolated through the Matrigel as it solidified. Gravity-induced flow across the middle Matrigel-filled channel resulted in aligned structures in Matrigel. (f) Additional media was added to the reservoirs before loading cells or further experiments.

the two outer channels were used for cell culture media. The microchannels were 250 μm in height and 1000 μm in width (Figure 1b) and the pillars (d = 100 μm) were spaced 100 μm apart from each other.

Figure 1c–f show the schematics of the preparation steps of the aligned Matrigel. First, the sterilized microfluidic device bonded to a glass coverslip was placed on a block of ice and allowed to equilibrate thermally before gel loading (Figure 1c). Matrigel is thermally sensitive and can be cross-linked rapidly at room temperature. Separately, Matrigel was thawed and maintained at 4 °C to be kept at the liquid state before being loaded into the microfluidic device using a pipet. Next, Matrigel was loaded into the middle channel and allowed to polymerize briefly for 5 min before 50 μL of media was added to one of the side channels (Figure 1d). To obtain aligned Matrigel, we applied constant flow during the gelation step. This was accomplished by simply tilting the entire device at a 90° angle, perpendicular to the substrate and allowing the media to flow across the gel-filled middle channel (Figure 1e, f).

Immediately following Matrigel injection into the microfluidic device, 50 μL of media was added to one of the side channels while keeping the opposite media channel empty. When the entire assembly was tilted at 90°, creeping flow across the pre-cross-linked Matrigel was generated (Figure 1c). Because the Matrigel was viscous and thick, it did not allow the media to flow readily from the top channel to the bottom channel. Media percolated through the gel as it became cross-linked and solidified.

To model this condition and to determine the presence of fluid flow inside the Matrigel that resulted in the alignment of ECM components, we used a commercial finite element method (FEM) solver. Figure 2a shows the result of the simulation over the entire device. The flow line across hydrogels was uniform and parallel near the middle region of the device. The fluid velocity showed varying magnitudes along the entire analysis area, but was largely constant around the middle region. Figure 2b shows a magnified image of the simulation results. Flow velocity profile and flow direction were influenced by the pillar structures. The fluid flow profile near the hexagonal pillars displayed a dissimilar tendency of the fluid flow in the middle of the microchannel. The flow velocity in the vicinity of pillars reached a maximum, while the flow was slow behind the pillars. The flow line diverged radially from the space between the pillars. The flow velocity and direction became uniform around 150 μm away from the top channel. Furthermore, the simulation of Matrigel showed deformation effects, such as sagging caused by gravity and the soft nature of Matrigel.

Figure 2c shows the graph of fluid flow velocity for two different fluids, Matrigel and water. We assumed that the fluids moved along the microchannel and simplified the microfluidic device into the spatially restricted zone to model the 3D single-phase flow. The flow of water and that of Matrigel in the spatially restricted zone were modeled independently. The two fluids moved with different velocities. Because of the viscous nature of Matrigel, it moved insignificantly along the flow direction, whereas water showed a faster flow velocity in the microfluidic channel. The relative movement between the water mode and the hydrogel mode caused frictional force that could be a source of shear stress as a deformation force. This fact indicated the role of shear flow in the alignment of the ECM components as Matrigel solidified.

Figure 2e and d show the simulation and experimental result of the cross-linked gel after exposure to fluid flow. Matrigel showed sagging between the posts, which was due to the effect of gravity and media flow. This phenomenon is shown in Figure 2d and was confirmed experimentally as shown in Figure 2e. Although the magnitudes of sagging are in slight disagreement, the presence of high flow velocity must exhibit an additional influence on top of the gravitational force.

Regions next to the pillars showed slow velocity profiles in contrast with the neighboring areas. However, approximately 150 μm away from the fluid/gel interface, the flow was well-developed and showed uniform velocity. This phenomenon was also confirmed in the experimental result shown in Figure 2e. The bright-field micrograph shows uniform parallel lines indicative of aligned ECM components.

Figure 3a–d shows bright-field images and fluorescently labeled images of the randomly cross-linked and flow-induced aligned Matrigel. When Matrigel was cross-linked in a microfluidic channel without flow, it showed a randomly structured morphology similar to that of a sponge. Both images show unorganized meshlike structures with irregular pores that could be found in conventional hydrogels.

In contrast, when Matrigel was cross-linked under constant exposure to flow, the gel showed aligned fibrous structures along the direction of flow. Both the dehydrated sample (Figure

DOI: 10.1021/am508292t
ACS Appl. Mater. Interfaces 2015, 7, 2183–2188

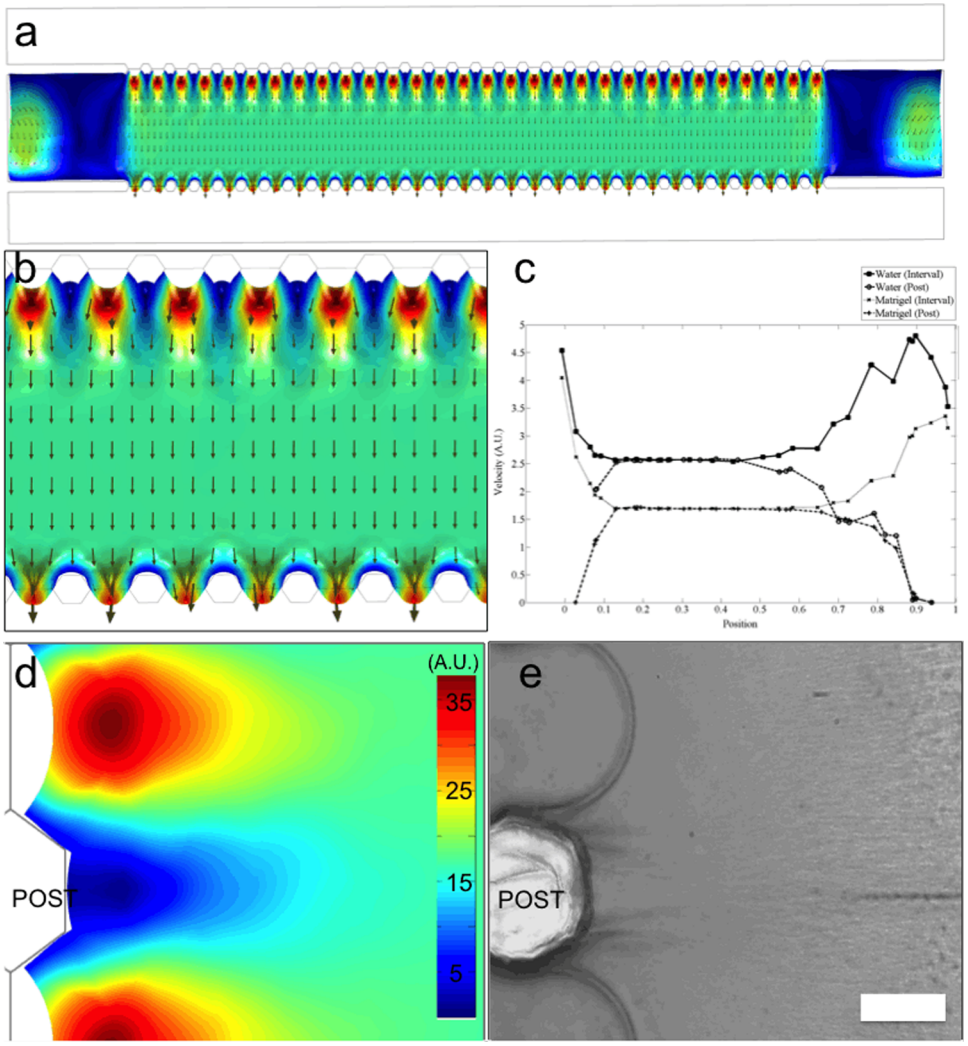

Figure 2. Simulation of the flow effects on the alignment of ECM components. (a, b) Flow simulation of gel in the tilted microfluidic device indicates that the media was soaked into the hydrogels and created flow inside gels through the center channel. (c) The pressure from the media volume in the microchannel created two types of flow and the mixed material across the Matrigel from the top to the bottom. And the velocity was acquired from two sections. One is a section between a post and the opposite post, another is a section between an interval and the opposite interval. The difference of each flow velocity at a height of 250 μm (a dotted line) means the shear flow across the Matrigel reorganized the cross-linking of the hydrogel during the gelling time. (d) The magnified image of the flow across the hydrogel at the initial position. The hydrogel experienced a large deflection under the pressure of media. (e) The experimental Matrigel was observed with the blue dye. Scale bar, 100 μm.

3c) and immunostained collagen IV (Figure 3d) showed starkly different morphologies compared with those of random gels, with finer and more elongated structures.

As described earlier, to generate flow across the gel, 50 μL of media was added to only one of the side channels and the whole device was tilted at 90°. However, the volume of liquid that traveled across the gel was significantly smaller than the total volume of media added. Most of the media remained in the original channel even after the gelation was completed. As a control experiment, no medium was added to the side channel, and the Matrigel-loaded sample was tilted at 90°. The absence of media did not generate flow or shear stress, and the resulting gel showed random sponge-like structures. The flow of Matrigel itself under the influence of gravity failed to generate aligned ECM components. This experiment confirmed the importance of shear stress because of continuous fluid flow across the gel.

Using the immunostained images (n = 10) of collagen IV similar to the ones shown in Figures 3b and 3d, the orientation of structures with respect to flow direction was analyzed. Figure 3e shows the graph of orientation angle for random and aligned Matrigel. As expected, randomly cross-linked Matrigel showed no preferred orientation in the structures while the aligned Matrigel showed a sharp peak centered along the direction of flow. Close to 70% of the structures showed preferred orientation within ±15° along the direction of flow.

In addition to the stained images of collagen IV, we wished to confirm the presence of aligned ECM components using an indirect approach. The cells were introduced into one of the side channels, plated on the gel after the Matrigel was injected into the microfluidic device, and solidified, as the ECM provides the cells with an environment for physical interaction and axonal outgrowth, in turn acting as proof of the oriented 3D gel environment.

Images a and b in Figure 4 show the schematic of the approach described in this section. We hypothesized that if the Matrigel contained aligned ECM components, they should direct the axonal outgrowth across the 1000 μm wide Matrigel channel. To test whether cell behavior is dependent on a single

DOI: 10.1021/am508292t
ACS Appl. Mater. Interfaces 2015, 7, 2183−2188

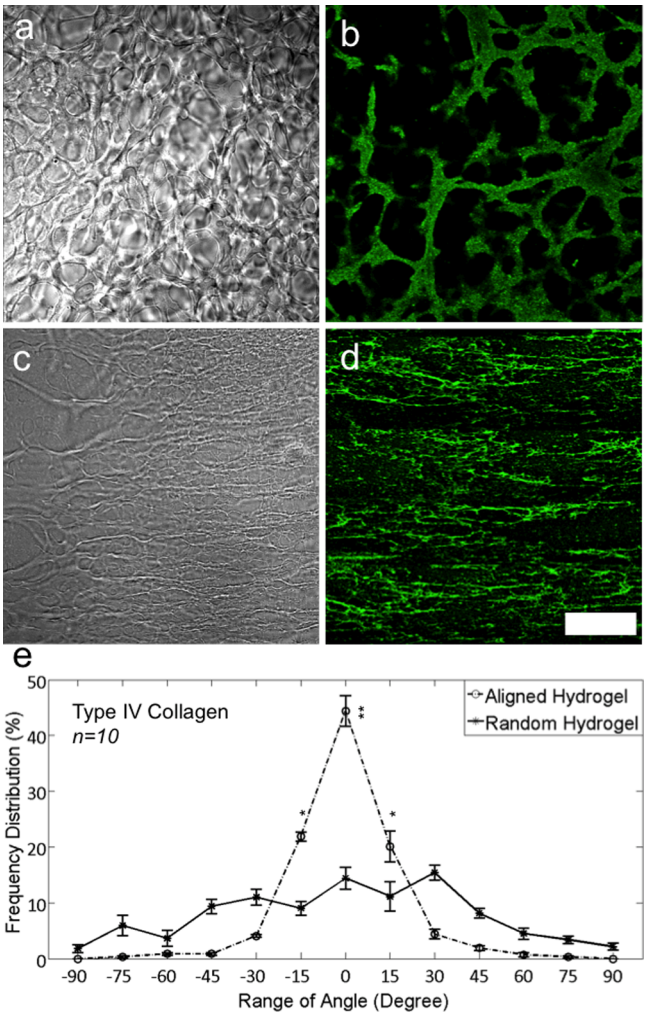

Figure 3. Bright-field images and fluorescently labeled images of the randomly cross-linked and flow-induced aligned Matrigel. (a) Dehydrated Matrigel cross-linked in a microfluidic channel showed random morphology. (b) Corresponding random gel was stained for collagen IV. The fluorescent micrograph shows similar random network structures of dehydrated gel. (c, d) When the Matrigel was cross-linked under constant exposure to flow, the network showed aligned structures. Dehydrated Matrigel and collagen IV showed aligned fibrous structures along the direction of flow. The structures were finer and more elongated than those of the randomly cross-linked Matrigel. (e) Graph of distribution over all angles to the flow direction shows the difference between nonfibrillar hydrogels without and with flow. Random hydrogels were distributed evenly over all angles (−90° to +90°). However, the flow-induced alignment of ECM components in Matrigel had high concentration at angles between −15° to +15°. In the flow-induced hydrogels, 70% of hydrogels were aligned (±15°) whereas the hydrogel without flow was distributed randomly (less than 20% for each angle). The numbers in the graph were calculated with MATLAB. Scale bar, 20 μm. Statistical comparisons were performed by t test; *P < 0.01, **P < 0.001.

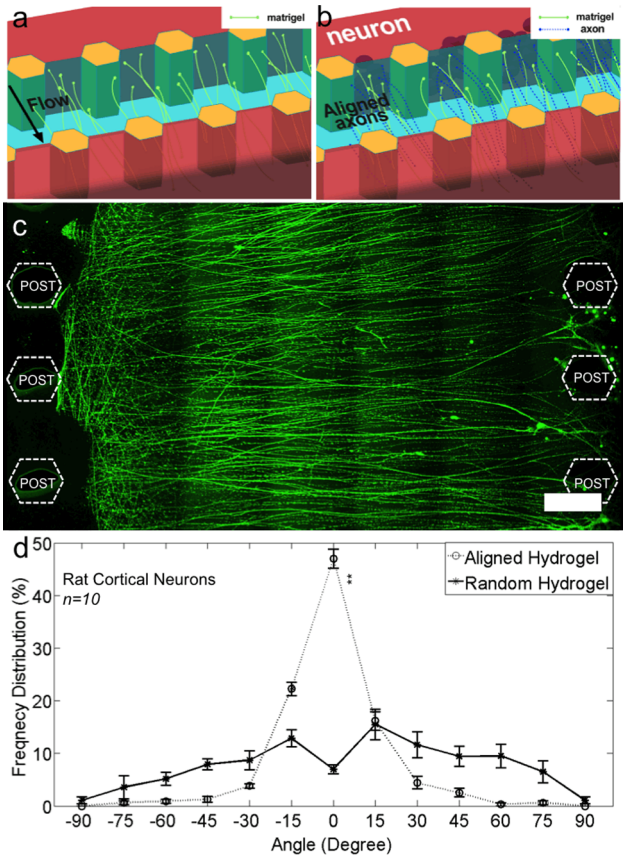

Figure 4. (a, b) Immunofluorescence image of β-tubulin representing axons derived from rat cortical neurons (12 days in vitro) and quantitative analysis of axonal alignment. The concept diagram aids in the understanding of the alignment of ECM components induced by shear flow and the axon alignment from rat cortical neurons (12 DIV) inside the Matrigel. (c) The immunofluorescence image of axon inside hydrogels in a microfluidic device indicates the hydrogel structure. Axons derived from rat (E17−18) grew randomly without flow across the Matrigel while axons were aligned in flow-induced hydrogels. (d) The results describe that the majority of axons in the aligned ECM components induced by flow grew in a straight fashion within the angle of ±15° compared with the results without flow. Scale bar, 200 μm. Statistical comparisons were performed by t test; **P < 0.001.

cell type, we used both primary rat cortical neurons that were plated as dissociated single cells and mouse neural stem cells that were plated into the device as neurospheres (diameter, ∼100−150 μm). The cells were introduced into the device. and the device was tilted to make the cells settle onto the side wall of the Matrigel.

Rat cortical neurons immunostained with class III β-tubulin antibody are shown in Figure 4c. The photograph was taken on 12 DIV, allowing enough time for the axons to project from the left side across the aligned Matrigel. For random cross-linked gels, the axons did not project in an orderly manner, and the total length of the neuronal processes was noticeably shorter than that of the aligned gels (not shown). Similar results were obtained for mouse neural stem cells (Figure S1, Supporting Information). Analysis of the orientation of neuronal processes along the direction of flow is shown in Figure 4d. Similar to the results obtained earlier for the orientation of the immunostained collagen IV, neuronal processes also showed preferred orientation along the direction of flow in the aligned gels. Close to 70% of the processes were aligned within ±15° along the direction of flow. As expected, the neuronal processes showed random orientations in random gels.

The flow in the microfluidic device was simulated, revealing that media flow created the shear flow that occurred rapidly across the hydrogel during polymerization. The simulation result of the flow direction was correlated with the experimental results. The flow model was simplified as a single-phasic flow model, and it was also assumed that no chemical reaction and

DOI: 10.1021/am508292t
ACS Appl. Mater. Interfaces 2015, 7, 2183−2188

no substantial entanglement occurred. Because Matrigel was thought to be a mixture of a solid polymer network and water, the two-phasic flow model for hydrated tissues, involving a solid phase and a liquid phase, could be employed. However, the phenomenon that we intended to simulate was the flow across hydrogels during gelation. The simulation of gelation with flow is one of the interesting problems involving rheology, which is beyond this work.

The experimental result showed that the flow rate was an important variable that exerts an influence on the alignment of ECM components in Matrigel. The degree of hydrogel alignment position close to a pillar or at the edge of microchannels became noticeably lower. The region was correlated with both the highest and lowest flow rate, as shown in the simulation results. Therefore, the hydrogel was thought to be aligned in the region of the flow velocity over a certain level. This fact alluded to the involvement of shear flow in hydrogel alignment, as the flow velocity was linearly proportional to the shearing deformation rate. In particular, major components in the hydrogel such as type IV collagen usually exhibit a complex branch network. Therefore, reforming them into anisotropic structures would demand mechanical stress over a certain level. However, the mechanical stress from gravity induced by tilting was not enough to deform or to break the polymer backbone, such as the perpendicular polymer networks, even though they were elastic and mechanically versatile. The noticeable event in our process was rather the gelation. The materials remained as viscous fluids before polymerization and flowed in company with the media along gravity. The relative movement between two other materials could prevent physical interaction perpendicular to the flow direction. The media trickled out from between the opposite pillars during the tilting process, and moved into the other microchannel while the Matrigel was stagnant in the microfluidic device. The simulation also resulted in different velocities of the two kinds of materials. These results meant that before Matrigel was randomly cross-linked, the relative movement worked as a kind of shear flow and determined the direction of polymerization. With the observation of these properties, we believe that the shear flow across the hydrogel could cause the deformation of the Matrigel without fibrillar networks along the direction of flow.

The goal of this study was to develop a robust method to align ECM components in hydrogels for use in 3D cell culture systems. We found that ECM components in 3D Matrigel could be assembled in an orderly aligned fashion by fluid flow. The gel alignment process was modeled using FEM modeling and compared with the experimental results. The shape and arrangement of immunostained collagen IV showed sharp contrasts between random and aligned gels. Large random networks of collagen IV were transformed into narrower and orderly aligned fibrous structures. In the indirect confirmation of the aligned ECM components, when rat cortical neurons were cultured, the axons and neuronal processes were preferentially oriented along the direction of flow. Our results implied a new technology to manipulate and impart alignment in 3D ECM structures with potential applications in 3D cell culture research. The method could be used to obtain gel alignment as effectively as other methods could, without the use of specialized machines and other materials. With further development, this method could serve as the basis for building organized neural networks in 3D.

■ ASSOCIATED CONTENT

Ⓢ Supporting Information

Immunofluorescence image of β-tubulin, GFAP derived from mouse neurospheres (5 days in vitro), and quantitative analysis of axonal alignment; image of axonal alignment at different height from rat cortical neurons in ECM alignment; procedure of fabrication, simulation, characterization of ECM component alignment, and primary cell culture. This material is available free of charge via the Internet at http://pubs.acs.org.

■ AUTHOR INFORMATION

Corresponding Author

*E-mail: njeon@snu.ac.kr. Telephone: +82-2-880-7111.

Present Address

Rm. #415−2, Bldg. 302, Seoul National University, Kwanak-ro 1, Kwanak-gu, Seoul, Korea

Author Contributions

[§]These authors contributed equally.

Notes

The authors declare no competing financial interest.

■ ACKNOWLEDGMENTS

We acknowledge funding from the Global Ph.D Fellowship Program (2011-006423), the Basic Science Research Program (2013R1A1A2006148), and the Brain Research Program (2012M3C7A1055413), Biomembrane Plasticity Research Center (2014051826) through the National Research Foundation of Korea (NRF).

■ ABBREVIATIONS

ECM, extra cellular matrix; FEM, finite element method

■ REFERENCES

(1) Gospodarowicz, D.; Delgado, D.; Vlodavsky, I. Permissive Effect of the Extracellular Matrix on Cell Proliferation in Vitro. *Proc. Natl. Acad. Sci. U.S.A.* **1980**, *77*, 4094−4098.

(2) Trappmann, B.; Gautrot, J. E.; Connelly, J. T.; Strange, D. G.; Li, Y.; Oyen, M. L.; Cohen Stuart, M. A.; Boehm, H.; Li, B.; Vogel, V.; Spatz, J. P.; Watt, F. M.; Huck, W. T. Extracellular-Matrix Tethering Regulates Stem-Cell Fate. *Nat. Mater.* **2012**, *11*, 642−649.

(3) Meredith, J. E., Jr.; Fazeli, B.; Schwartz, M. A. The Extracellular Matrix as a Cell Survival Factor. *Mol. Biol. Cell* **1993**, *4*, 953−961.

(4) Daley, W. P.; Peters, S. B.; Larsen, M. Extracellular Matrix Dynamics in Development and Regenerative Medicine. *J. Cell Sci.* **2008**, *121*, 255−264.

(5) Kleinman, H. K.; Martin, G. R. Matrigel: Basement Membrane Matrix with Biological Activity. *Semin. Cancer Biol.* **2005**, *15*, 378−386.

(6) Cukierman, E.; Pankov, R.; Stevens, D. R.; Yamada, K. M. Taking Cell-Matrix Adhesions to the Third Dimension. *Science* **2001**, *294*, 1708−1712.

(7) Khademhosseini, A.; Langer, R. Microengineered Hydrogels for Tissue Engineering. *Biomaterials* **2007**, *28*, 5087−5092.

(8) Tibbitt, M. W.; Anseth, K. S. Hydrogels as Extracellular Matrix Mimics for 3d Cell Culture. *Biotechnol. Bioeng.* **2009**, *103*, 655−663.

(9) Liu, D.; Bastiaansen, C. W.; den Toonder, J. M.; Broer, D. J. (Photo-)Thermally Induced Formation of Dynamic Surface Topographies in Polymer Hydrogel Networks. *Langmuir* **2013**, *29*, 5622−5629.

(10) Bryant, S. J.; Cuy, J. L.; Hauch, K. D.; Ratner, B. D. Photo-Patterning of Porous Hydrogels for Tissue Engineering. *Biomaterials* **2007**, *28*, 2978−2986.

(11) Luo, Y.; Shoichet, M. S. A Photolabile Hydrogel for Guided Three-Dimensional Cell Growth and Migration. *Nat. Mater.* **2004**, *3*, 249−253.

DOI: 10.1021/am508292t
ACS Appl. Mater. Interfaces 2015, 7, 2183−2188

(12) Bian, W.; Bursac, N. Engineered Skeletal Muscle Tissue Networks with Controllable Architecture. *Biomaterials* **2009**, *30*, 1401−1412.
(13) Johansson, F.; Carlberg, P.; Danielsen, N.; Montelius, L.; Kanje, M. Axonal Outgrowth on Nano-Imprinted Patterns. *Biomaterials* **2006**, *27*, 1251−1258.
(14) Murphy, S. V.; Atala, A. 3d Bioprinting of Tissues and Organs. *Nat. Biotechnol.* **2014**, *32*, 773−785.
(15) Dhariwala, B.; Hunt, E.; Boland, T. Rapid Prototyping of Tissue-Engineering Constructs, Using Photopolymerizable Hydrogels and Stereolithography. *Tissue Eng.* **2004**, *10*, 1316−1322.
(16) Chan, V.; Zorlutuna, P.; Jeong, J. H.; Kong, H.; Bashir, R. Three-Dimensional Photopatterning of Hydrogels Using Stereolithography for Long-Term Cell Encapsulation. *Lab Chip* **2010**, *10*, 2062−2070.
(17) Lee, S. H.; Moon, J. J.; West, J. L. Three-Dimensional Micropatterning of Bioactive Hydrogels Via Two-Photon Laser Scanning Photolithography for Guided 3d Cell Migration. *Biomaterials* **2008**, *29*, 2962−2968.
(18) Ekaputra, A. K.; Prestwich, G. D.; Cool, S. M.; Hutmacher, D. W. Combining Electrospun Scaffolds with Electrosprayed Hydrogels Leads to Three-Dimensional Cellularization of Hybrid Constructs. *Biomacromolecules* **2008**, *9*, 2097−2103.
(19) Xu, F.; Wu, C. A.; Rengarajan, V.; Finley, T. D.; Keles, H. O.; Sung, Y.; Li, B.; Gurkan, U. A.; Demirci, U. Three-Dimensional Magnetic Assembly of Microscale Hydrogels. *Adv. Mater.* **2011**, *23*, 4254−4260.
(20) Cheng, X.; Gurkan, U. A.; Dehen, C. J.; Tate, M. P.; Hillhouse, H. W.; Simpson, G. J.; Akkus, O. An Electrochemical Fabrication Process for the Assembly of Anisotropically Oriented Collagen Bundles. *Biomaterials* **2008**, *29*, 3278−3288.
(21) Lanfer, B.; Freudenberg, U.; Zimmermann, R.; Stamov, D.; Korber, V.; Werner, C. Aligned Fibrillar Collagen Matrices Obtained by Shear Flow Deposition. *Biomaterials* **2008**, *29*, 3888−3895.
(22) Tanaka, Y.; Kubota, A.; Matsusaki, M.; Duncan, T.; Hatakeyama, Y.; Fukuyama, K.; Quantock, A. J.; Yamato, M.; Akashi, M.; Nishida, K. Anisotropic Mechanical Properties of Collagen Hydrogels Induced by Uniaxial-Flow for Ocular Applications. *J. Biomater. Sci., Polym. Ed.* **2011**, *22*, 1427−1442.
(23) Cosson, S.; Allazetta, S.; Lutolf, M. P. Patterning Of Cell-Instructive Hydrogels By Hydrodynamic Flow Focusing. *Lab Chip* **2013**, *13*, 2099−2105.
(24) Guo, C.; Kaufman, L. J. Flow and Magnetic Field Induced Collagen Alignment. *Biomaterials* **2007**, *28*, 1105−1114.
(25) Pregibon, D. C.; Toner, M.; Doyle, P. S. Magnetically and Biologically Active Bead-Patterned Hydrogels. *Langmuir* **2006**, *22*, 5122−5128.
(26) Rakickas, T.; Ericsson, E. M.; Ruzele, Z.; Liedberg, B.; Valiokas, R. Functional Hydrogel Density Patterns Fabricated by Dip-Pen Nanolithography and Photografting. *Small* **2011**, *7*, 2153−2157.
(27) Lee, M. K.; Rich, M. H.; Shkumatov, A.; Jeong, J. H.; Boppart, M. D.; Bashir, R.; Gillette, M. U.; Lee, J.; Kong, H. Glacier Moraine Formation-Mimicking Colloidal Particle Assembly in Microchanneled, Bioactive Hydrogel for Guided Vascular Network Construction. *Adv. Healthcare Mater.* **2014**, DOI: 10.1002/adhm.201400153.
(28) East, E.; de Oliveira, D. B.; Golding, J. P.; Phillips, J. B. Alignment of Astrocytes Increases Neuronal Growth in Three-Dimensional Collagen Gels and Is Maintained Following Plastic Compression to Form a Spinal Cord Repair Conduit. *Tissue Eng., Part A* **2010**, *16*, 3173−3184.
(29) Odawara, A.; Gotoh, M.; Suzuki, I. A Three-Dimensional Neuronal Culture Technique That Controls the Direction of Neurite Elongation and the Position of Soma to Mimic the Layered Structure of the Brain. *RSC Adv.* **2013**, *3*, 23620.
(30) Huang, C. P.; Lu, J.; Seon, H.; Lee, A. P.; Flanagan, L. A.; Kim, H. Y.; Putnam, A. J.; Jeon, N. L. Engineering Microscale Cellular Niches for Three-Dimensional Multicellular Co-Cultures. *Lab Chip* **2009**, *9*, 1740−1748.

DOI: 10.1021/am508292t
ACS Appl. Mater. Interfaces 2015, 7, 2183−2188